IOP Conf. Series: Materials Science and Engineering **1350** (2026) 012001 doi:10.1088/1757-899X/1350/1/012001

Evolution and cessation of the bainite transformation

H K D H Bhadeshia

School of Materials Science & Engineering,
Queen Mary University of London, U. K.

E-mail: h.bhadeshia@qmul.ac.uk

Abstract. Real-time studies of solid-state transformations have reached unprecedented levels of detail. In bainite (α_b), the use of synchrotron, neutron, and atom probe tomography facilities has demonstrated that parent austenite (γ) remains chemically and structurally unperturbed prior to transformation. This disproves the long-held notion of precursor fluctuations, which are fundamentally inconsistent with the thermodynamics of the γ solid solution. Although not 'real-time', atomic force microscopy too, has played a seminal role in establishing reality.

Experiments show that α_b possesses tetragonal symmetry, resulting in anisotropic thermal expansion, leading to a revised Fe–C phase diagram. *In situ* lattice parameter measurements during tempering reveal that specific austenite morphologies exhibit enhanced thermal stability. The high-resolution techniques also explain the divergence between the excellent fracture toughness (K_{IC}) and yet, poor Charpy impact resistance of strong bainite. Finally, 150 independent experiments confirm that the bainite reaction ceases when diffusionless transformation is no longer thermodynamically possible.

1 Carbon concentration fluctuations

Some have taken the partitioning of carbon observed following the bainite transformation to imply that the austenite first becomes compositionally unstable and separates into carbon-rich and carbon-depleted volumes. This would be akin to the uphill diffusion observed during spinodal reactions [1]. Under this hypothesis, the low-carbon regions are supposed to transform into supersaturated bainite of the same composition via a 'martensite-like' lattice rearrangement.

However, Aaronson [2] showed that this mechanism is inconsistent with the thermodynamics of an austenitic Fe-C solid solution. The concept nonetheless seems to crop up with notorious regularity [3–5]. X-ray *in-situ* experiments using synchrotron facilities appeared, at one stage, to indicate that the austenite unit cell splits into two identical lattices with different lattice parameters prior to the onset of the bainite transformation [6, 7]. Subsequently, higher-resolution experiments established that these reports were based on an incorrect analysis of limited X-ray data; the austenite remains homogeneous with a unique lattice parameter prior to transformation into bainite, as shown in figure 1 [8]. Neutron and other X-ray diffraction experiments have since confirmed this conclusion, failing to find an austenite diffraction peak splitting prior to transformation [9–13].

This does not rule out random compositional fluctuations typical of any solution in dynamic equilibrium at a non-zero temperature. While it has been argued that such fluctuations favour nucleation in momentarily depleted regions of austenite [14], this does not change the reality that the solution is *thermodynamically homogeneous* on an observable scale. Indeed, carbon-depleted regions containing several thousand iron atoms can temporarily exist at all temperatures in austenite of eutectoid composition [15]. However, for every such region, there must also exist a carbon-enriched volume where the probability of ferrite nucleation is reduced, thereby balancing the overall effect of the depleted regions.

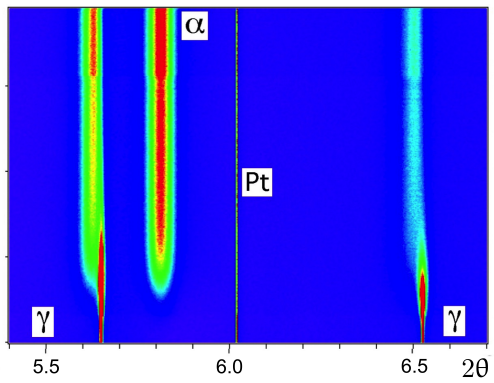

(a) Transformation at 300 °C, showing that the austenite has a unique lattice parameter prior to the formation of carbide-free bainite.

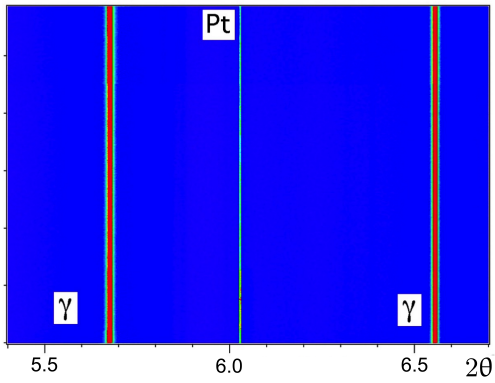

(b) Holding at 200 °C for ten hours prior to the onset of bainite, showing the absence of any peak splitting. After [8].

Figure 1. X-ray diffraction during isothermal holding. The vertical scale represents the progress of time; blue and red represent low and high intensities respectively.

While some attribute bainite nucleation to carbon-depleted zones near dislocations [16], this view overlooks the high mobility of carbon in austenite. At the dimensions typical of a nucleation event, diffusion is sufficiently rapid to equilibrate any such gradients.

2 Carbon retained in tetragonal, supersaturated bainitic-ferrite plates

It is now generally accepted that the $\gamma \rightarrow \alpha_b$ transformation is displacive [17]. Atomic force microscopy has shown that the growth of a thin-platelet ('subunit') that cannot be resolved using visible light, is accompanied by an invariant-plane strain shape deformation with a shear strain parallel to the habit plane of $s \approx 0.26$, and a dilatational strain normal to that plane of $\xi \approx 0.03$ [18], figure 2a. A clever experiment using a focussed ion beam two machine two non-parallel surfaces that meet at an edge, then examined using an atomic force microscope, has proven that the α_b-subunits seen in two-dimensional sections, are in fact plates in three dimensions, figure 2b [19]. This precisely is consistent with the observed shape deformation because a thin-plate shape reduces the consequential strain energy [20]. In fact, this remains the only explanation for the plate shapes of Widmanstätten ferrite, bainite and martensite [17].

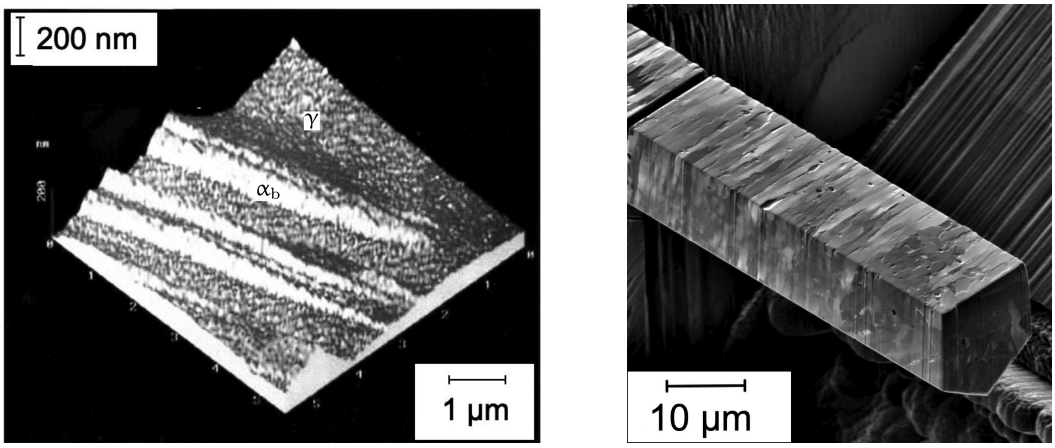

(a) **(b)**

Figure 2. (a) Atomic force microscope image of the displacements caused by individual, lenticular platelets of bainite at the free surface of austenite [18]. (b) Two-surface image showing the α_b plate-shape in three dimensions (reproduced with permission of Elsevier, from Costin et al. [19]).

There is overwhelming evidence that when the carbon in austenite remains in solid solution, the bainite transformation is **halted** when the concentration reaches a value where austenite and ferrite of the same composition have identical free energies [Fig. 2, 17]. In other words, the transformation is diffusionless with carbon partitioning occurring after growth, effectively an auto-tempering process first suggested by Hehemann [21].

There are some remarkable remnants of the diffusionless growth of bainite, which came to light using the atom probe. The carbon concentration that persists in bainitic ferrite even after some has partitioned into the residual austenite, is much in excess of equilibrium. This originally was assumed to be due to segregation to dislocations [22–29]. Vasudevan et al. [30] using chemical analysis revealed supersaturated bainitic ferrite as long ago as 1958. Later work Pereloma et al. and Caballero et al. showed that the persistent carbon is in fact in solid solution [31–33], figure 3a and remains there even after 250 h at 200 °C, so it is not mobility that stops the carbon from partitioning into the residual-γ.

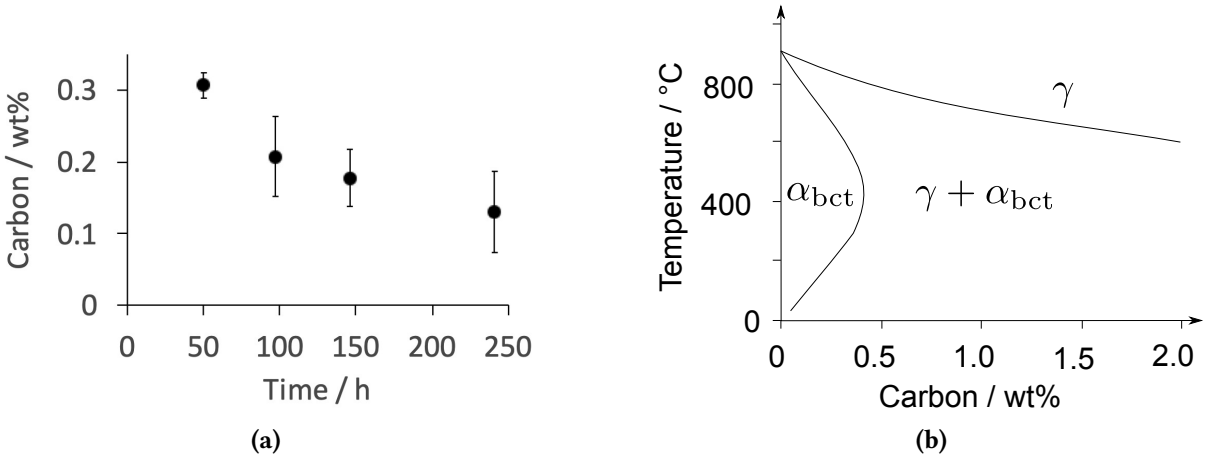

(a) **(b)**

Figure 3. (a) Carbon dissolved in α_b during holding at 200 °C [34]. (b) Fe-C phase diagram for the equilibrium between body-centred tetragonal α and γ [35].

Synchrotron X-ray experiments [36, 37] first demonstrated that α_b containing excess carbon ex-

hibits a tetragonal (α_b^{bct}) rather than cubic symmetry, though these data have now been confirmed using a variety of techniques [38–45]. The tetragonal symmetry which changed continuously when the sample was *in situ* heated from the transformation temperature [36, 37]. A wealth of information entirely unexpected, has emerged, such as the characterisation of anisotropic thermal expansion of α_b as a function of temperature, again using synchrotron X-rays [38].

The relevant equilibrium in these circumstances is between α_b^{bct} and γ, not that between cubic-ferrite and γ. Figure 3b shows a calculated Fe-C diagram for the α^{bct}/γ equilibrium [35]; the solubility of carbon is increased significantly, explaining the large concentration that persists within α_b^{bct}.

Alternatively, carbon atoms have been suggested to associate with host vacancies in the α_b, thus compromising their mobility [46], but in fact the fraction of those atoms that pair with host vacancies is negligibly small [47], [pp. 117-119, 48].

3 Photoemission electron microscopy

What optically appears to be a single plate of bainite, in fact consists of an aggregate of fine platelets (the sheaves) that share a common crystallographic orientation [Fig. 1, 49]. These subunits are typically $\approx$ 0.2 µm thick, but can be as thin as 20 nm — these cannot be resolved using optical or confocal-laser microscopy. All plate-lengthening experiments based on these techniques therefore do not have the resolution to measure the growth of individual subunits, but rather, focus on the growth rate of sheaves, which necessarily is slower [equation 6.31, 50]. A photoemission electron microscope can resolve individual subunits as they grow. The lengthening rate thus measured (figure 4) is many orders of magnitude greater than that calculated assuming paraequilibrium at the transformation front (*cf.* 75 µm s^{-1} measured and 0.083 µm s^{-1} calculated assuming carbon diffusion-controlled lengthening).

4 Acoustic emissions

Acoustic emissions are transient elastic waves generated by the rapid release of energy from localised sources within a material. When a solid-state phase transformation occurs, the lattice shifts, often creating a pulse of energy that travels to the surface as a sound wave. These emissions are manifestations of abrupt changes in the internal stress field [52] and are, therefore, fundamentally consistent with displacive transformations. These waves can be converted into electrical signals using appropriate piezoelectric transducers.

Rapid, displacive transformations generate acoustic emissions that are absent during reconstructive transformations [53–55]. Interestingly, the frequency of emissions is significantly higher for bainite than for martensite [figure 5, 56], implying that the mean lifetime of individual emission events is shorter for bainite. These signals are interpreted as the result of dislocation sources triggered by the displacive strain. The motion of the bainite-austenite interface is relatively jerky due to the sub-unit mechanism of growth, which results in a smaller mean free path for interfacial dislocations compared to the long-range growth of martensite plates.

Since the original studies, several reports have confirmed acoustic emissions during the rapid formation of bainite or bainite containing a midrib of thin-plate martensite [57–59]. In these cases, signals are often stronger when associated with martensitic transformation; this is expected, given that higher transformation temperatures for bainite increase anelastic attenuation, which dampens the acoustic signal.

During continuous cooling transformation, acoustic emissions have been used to map the transition from Widmanstätten ferrite (which is a carbon diffusion-controlled displacive transformation [48, 60] but 'quieter') to bainite [61]. In further experiments on the same steel [62], a clear distinction was possible between displacive and reconstructive transformations, using a modified dilatometer equipped with an acoustic emission waveguide covering a wide band of frequencies (20-900 kHz). Dilatometric length

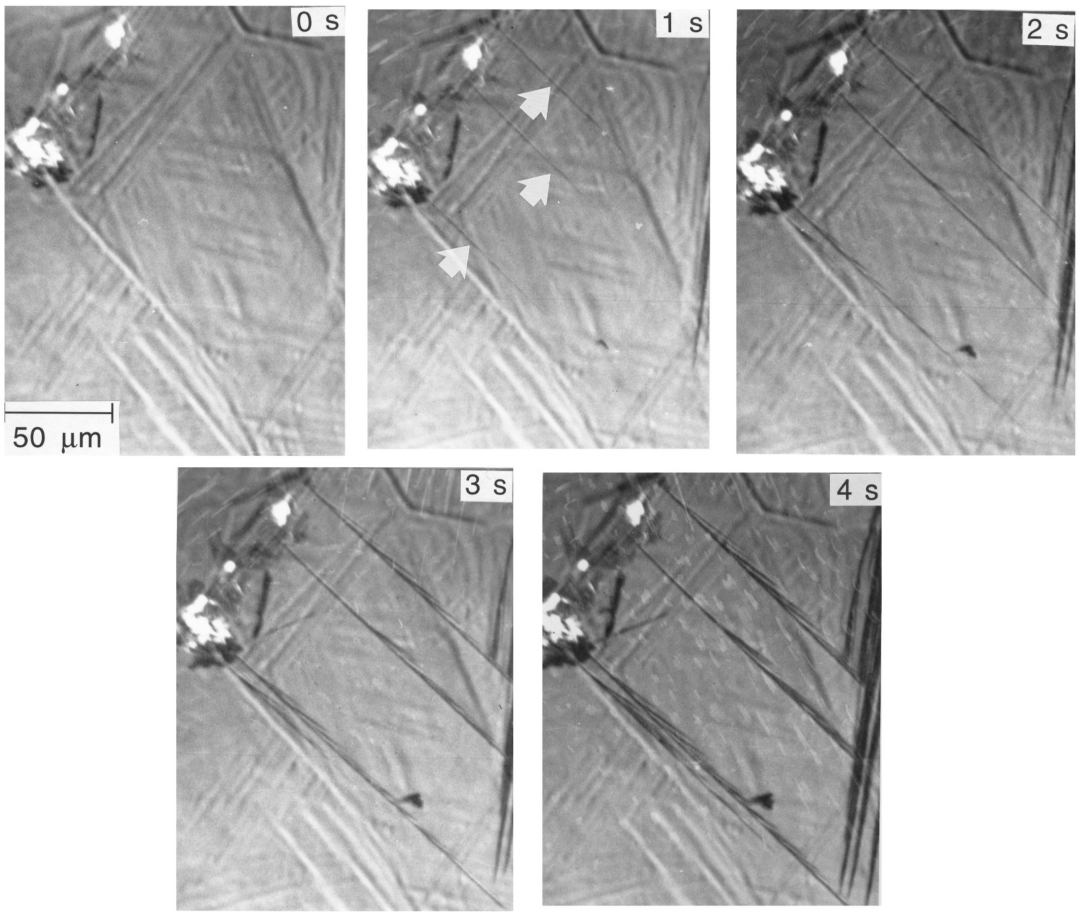

Figure 4. Photoemission electron microscope observations on the growth of individual sub-units in a bainite sheaf [51]. The pictures are taken at 1 s intervals during transformation at 380 °C in a Fe-0.43C-2.02Si-3Mn wt% alloy. The micrograph at 0 s is fully austenitic, the relief being a residue from an earlier experiment.

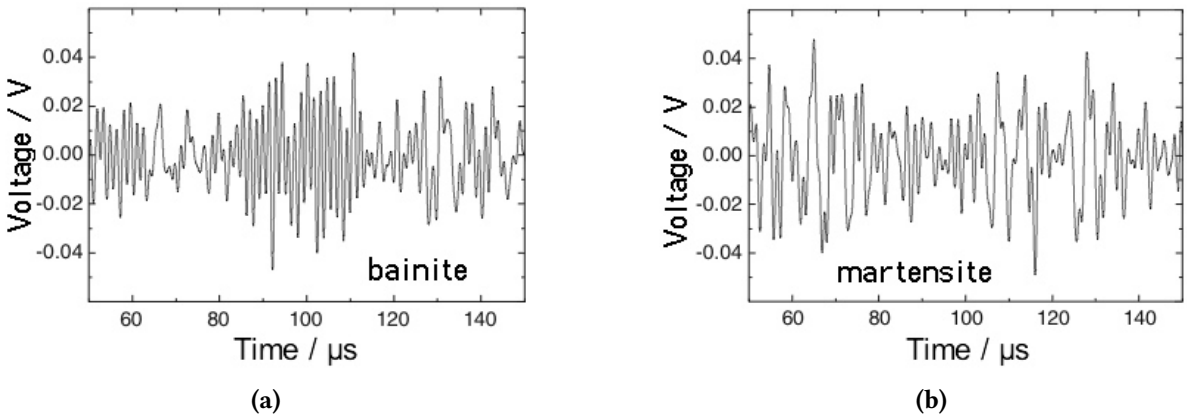

Figure 5. Acoustic emission signal from bainite and from martensite. Reproduced with permission from Taylor and Francis Ltd, http://www.tandfonline.com from Bohemen et al. [56].

changes due to ferrite formation did not lead to acoustic signals beyond the background noise. But when bainite formed, the sensors recorded distinct acoustic burst events.

In a notable study, Kuba and van Aken [63] characterised acoustic emissions during the rapid melting of indium-rich particles in an aluminium matrix. This melting involves a volume change comparable to phase transformations in steels. They demonstrated that while acoustic emissions are not strictly exclusive to displacive transformations, a significant volume change only generates detectable signals if the relaxation of the product phase occurs in less than 10^{-5} s. Such a timescale is inconsistent with reconstructive transformations in iron, but is entirely consistent with the rapid growth of bainite subunits. Consequently, the detection of acoustic emissions during bainitic transformation, and their absence during reconstructive growth, provides further support for the speed of the phase change.

An important conclusion from research into acoustic emissions is that it remains perhaps the most sensitive *in situ* technique available for defining the initiation of bainite during isothermal heat treatment [64]. The elastic strain energy resulting from the shape deformation is approximately $400\,\mathrm{J\,mol^{-1}}$ (equivalent to $56.4\,\mathrm{MJ\,m^{-3}}$). Given that the volume of an individual subunit is typically $\approx 2\times10^{-17}\,\mathrm{m^3}$ (for a subunit $0.2\,\mu\mathrm{m}$ thick and $10\,\mu\mathrm{m}$ long), the total elastic energy associated with a single subunit is $\approx 1.1\,\mathrm{nJ}$.

However, only a small fraction (0.01–1%) of this energy is released as detectable acoustic emission [65]. Since recorded emission events for bainite are typically in the range of 1–10 nJ [64], it is highly unlikely that a one-to-one correspondence exists between a single acoustic event and the formation of an individual bainite subunit. Instead, these emissions represent a stochastic measure of the transformation rate, capturing the collective, rapid formation of subunit clusters or sheaves, rather than acting as a literal counter for individual platelets.

5 Austenite shape and thermal stability

Carbide–free bainitic steels, characterised by a structure of bainitic ferrite and carbon–enriched retained austenite (γ_r), are established as sophisticated engineering materials. Their applications are diverse, spanning formable automotive alloys [66, 67], ductile cast irons [68], railway tracks [69, 70], and armour [71–75].

Retained austenite primarily enhances ductility by transforming under stress or strain [76, 77]. This transformation increases the work–hardening rate, thereby delaying plastic instability; however, the *transformation strain* itself contributes only marginally to this effect [78]. Understanding and controlling the mechanical stability of austenite remains central to tailoring the mechanical properties of these steels. This mechanical stability is affected by the tempering of $\alpha_b + \gamma$ because the enriched-austenite may decompose wholly or in part into cementite:

$$\gamma_r \xrightarrow{\text{temper}} \gamma_r + \theta + \alpha_b \xrightarrow{\text{cool}} \gamma_r + \theta + \alpha_b + \alpha'$$

where α' refers to martensite. It turns out, that the shape and the size of the austenite domains matters. There are two morphologies of austenite, the blocks and the thin films trapped between the platelets of bainitic ferrite. The films are known from independent experiments to be more mechanically stable to martensitic transformation [79] and are richer in carbon [22, 80, 81]. The two kinds of γ_r can therefore be distinguished by their lattice parameters during diffraction experiments. Figure 6 shows vividly that the films of austenite are less stable when tempered to precipitate cementite.

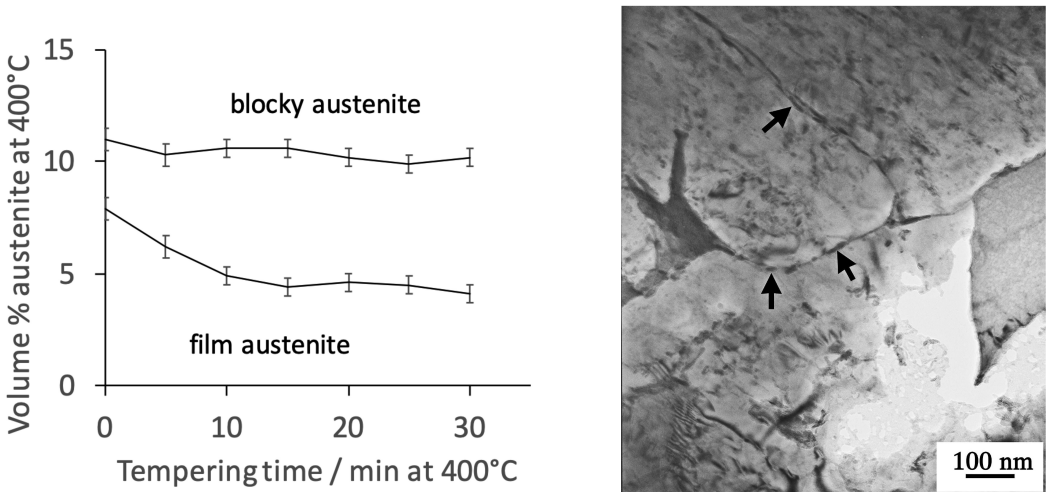

Figure 6. (a) Synchrotron monitoring of phase changes in Fe-0.39C-4.09Ni-2.05Si wt% during tempering at 400 °C [81]. Note: cooling to ambient temperature induces martensitic transformation, decoupling measurements from high-temperature carbide precipitation. (b) Micrograph showing cementite after 30 min at 400 °C [81].

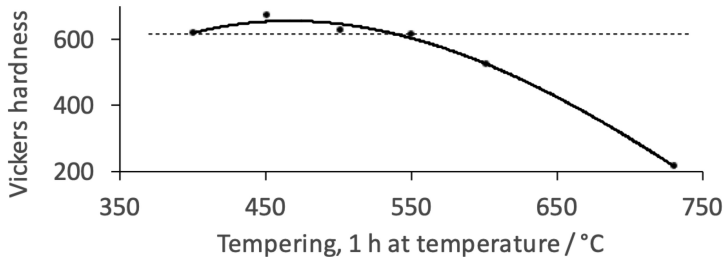

Figure 7. Tempering response of nanostructured α_b + γ in Fe-0.98C-1.46Si-1.89Mn-1.26Cr-0.26Mo-0.09V wt% [82].

In summary, while carbon-rich films of austenite effectively resist martensitic transformation during deformation, they exhibit lower thermal stability than blocky austenite during tempering. The rapid precipitation of cementite within these films (figure 7) can be so extensive that the resulting dispersion hardening offsets the loss of austenite, leading to a negligible change in overall hardness [82].

6 Toughness anomalies

Remarkably, nanostructured bainite can exhibit poor Charpy impact toughness despite possessing high fracture toughness (K_{IC}). High-resolution synchrotron X-ray diffraction has been utilised to characterise the notch root regions of nanostructured bainitic Charpy specimens, both in the as-machined state and after loading. This enabled the quantification of austenite fraction evolution during three-point bending. Analysis of diffraction peak shifts further revealed the distribution of residual tensile and compressive strains resulting from machining and subsequent loading. The findings indicate that the poor Charpy performance stems from the formation of stress-induced martensite at the notch root prior to crack initiation [83], effectively embrittling the region where the fracture starts.

7 Conclusions

Our understanding of the bainite transformation has been assisted by *in situ* observations, some of which are listed in Table 1. Synchrotron X-ray and neutron diffraction have settled debates by proving that austenite remains chemically homogeneous prior to transformation, while also revealing a persistent tetragonality in bainitic ferrite that stimulates another interpretation of the Fe–C phase diagram. The application of atomic force microscopy and photoemission electron microscopy has provided direct, three-dimensional proof of the plate-like morphology and the rapid, displacive nature of subunit growth, which far exceeds rates predicted by diffusion-controlled models. Collectively, these methods, including the sensitive detection of elastic energy via acoustic emissions, confirm that the nature of the bainite reaction to a point where educated steel design becomes quantitative.

Table 1: Experimental discoveries and their implications for the bainite transformation.

Method	Observation	Significance
Synchrotron X-ray, neutron diffraction	Unique γ lattice parameter prior to transformation	No precursor carbon fluctuations.
Atom-probe tomography, synchrotron	Persistent excess carbon in α_b and tetragonality	Confirms asymmetry, interpretation of phase diagrams.
Atomic-force microscopy	Invariant-plane strain shape deformation	Establishes deformation due to α_b, 3D plate morphology of subunits.
Photoemission electron microscopy	Lengthening rate of individual subunits	Growth too fast for carbon diffusion-controlled mechanisms.
Acoustic emissions	Detectable acoustic bursts during transformation	Signals rapid energy release consistent with growth mechanism.
In situ synchrotron tempering	Morphology-dependent austenite decomposition	Film austenite thermally less stable than blocky variety.

Acknowledgement: I am grateful to the organisers of this meeting for the opportunity to participate, and to the many metallurgists, referred to in context.

References

[1] Hilliard J E 1970 Spinodal decomposition *Phase Transformations* ed Zackay V F and Aaronson H I (Metals Park, Ohio, USA: ASM International) pp 497–560
[2] Aaronson H I, Domian H A and Pound G M 1966 *TMS-AIME* **236** 753–767
[3] Prado J M 1986 *Journal of Materials Science Letters* **5** 1075–1076
[4] Prado J M, Catalan J J and Marsal M 1990 *Journal of Materials Science* **25** 1939–1946
[5] Kang M, Zhu M and Zhang M 2005 *Journal of Materials Science and Technology* **21** 437–444
[6] Babu S S, Specht E D, David S A, Karapetrova E, Zschack P, Peet M and Bhadeshia H K D H 2005 *Metallurgical & Materials Transactions A* **36A** 3281–3289
[7] Babu S S, Specht E D, David S A, Karapetrova E, Zschack P, Peet M and Bhadeshia H K D H 2007 Time-resolved X-ray diffraction investigation of austenite and transformation to bainite *1st International Symposium on Steel Science* ed Tsuzaki K and Furuhara T Iron and Steel Institute of Japan (Tokyo, Japan: Iron and Steel Institute of Japan) pp 93–99

[8] Stone H J, Peet M J, Bhadeshia H K D H, Withers P J, Babu S S and Specht E D 2008 *Proceedings of the Royal Society A* **464** 1009–1027 ISSN 1364-5021
[9] Koo M, Xu P, Tomota Y and Suzuki H 2009 *Scripta Materialia* **61** 797–800
[10] Onuki Y, Umemura K, Fujiwara K, Tanaka Y, Tomida T, Kawano K and Sato S 2022 *Metals* **12** 957
[11] Zhou L, Fang F, Kumagai M, Pickering E, Yu T and Zhang X 2022 *Scripta Materialia* **215** 114696
[12] Wang Y, Tomota Y, Ohmura T, Gong W and Harjo S 2023 *Materialia* **27** 101685
[13] Tomota Y, Harjo S, Xu P, Morooka S, Gong W and Wang Y 2025 *Metals* **15** 610
[14] Yu D, Chen D, Zheng J, He Y and Shen F 1989 *Acta Metallurgica Sinica* **2** 161–167
[15] Russell K C 1971 *Metallurgical Transactions* **2** 5–12
[16] Zhao S X, Wang W and Mao D L 2007 *Key Engineering Materials* **334-335** 121–124
[17] Bhadeshia H K D H 2026 *Metallurgical & Materials Transactions A* **57** 1–20
[18] Swallow E and Bhadeshia H K D H 1996 *Materials Science and Technology* **12** 121–125
[19] Costin W L, Lavigne O and Kotousov A 2016 *Materials Science & Engineering A* **663** 193–203
[20] Christian J W 1958 *Acta Metallurgica* **6** 377–379
[21] Hehemann R F 1970 The bainite transformation *Phase Transformations* ed Aaronson H I and Zackay V F (Materials Park, Ohio, USA: American Society of Materials) pp 397–432
[22] Bhadeshia H K D H and Waugh A R 1982 *Acta Metallurgica* **30** 775–784
[23] Bhadeshia H K D H and Waugh A R 1982 An atom-probe study of bainite *Solid-Solid Phase Transformations* ed Aaronson H I, Laughlin D E, Sekerka R F and Wayman C M (Warrendale, Pennsylvania, USA: TMS-AIME) pp 993–998
[24] Stark I, Smith G D W and Bhadeshia H K D H 1988 The element distribution associated with the incomplete reaction phenomenon in steels: an atom probe study *Phase Transformations '87* ed Lorimer G E (London, U.K.: Institute of Metals) pp 211–215
[25] Peet M, Babu S S, Miller M K and Bhadeshia H K D H 2004 *Scripta Materialia* **50** 1277–1281
[26] Bruna P, Pradell T, Crespo D, Garcia-Mateo C and Bhadeshia H K D H 2005 Mössbauer spectroscopy of low temperature bainite *Industrial Applications of the Mössbauer Effect* ed Garcia M, Marco J F and Plazaola F (Maryland, U.S.A.: American Institute of Physics) pp 338–343
[27] Caballero F G, Miller M K, Babu S S and Garcia-Mateo C 2007 *Acta Materialia* **55** 381–390
[28] Pereloma E V, Timokhina E V, Miller M K and Hodgson P D 2007 *Acta Materialia* **55** 2587–2598
[29] Caballero F G, Miller M K and Mateo C G 2014 *Materials Science and Technology* **30** 1034–1039
[30] Vasudevan P, Graham L W and Axon H J 1958 *Journal of the Iron and Steel Institute* **190** 386–391
[31] Pereloma E, Beladi H, Zhang L and Timokhina I 2012 *Metallurgical & Materials Transactions A* **43** 3958–3971
[32] Caballero F G, Miller M K, Garcia-Mateo C and Cornide J 2013 *Journal of Alloys and Compounds* **577** S626–S630
[33] Pushkareva I, Macchi J, Shalchi-Amirkhiz B, Fazeli F, Geandier G, Danoix F, Teixeira J D C, Allain S Y P and Scott C 2023 *Scripta Materialia* **224** 115140
[34] Garcia-Mateo C, Jimenez J A, Yen H W, Morales-Rivas L, Kuntz M, Ringer S P, Yang J R and Caballero F G 2015 *Acta Materialia* **91** 162–173
[35] Jang J H, Bhadeshia H K D H and Suh D W 2012 *Scripta Materialia* **68** 195–198
[36] Hulme-Smith C N, Lonardelli I, Dippel A C and Bhadeshia H K D H 2013 *Scripta Materialia* **69** 409–412
[37] Hulme-Smith C N, Peet M J, Lonardelli I, Dippel A C and Bhadeshia H K D H 2015 *Materials Science and Technology* **31** 254–256
[38] Dutta R K, Huizenga R M, Amirthalingam M, Gao H, King A, Hermans M J M and Richardson I M 2014 *Materials Science Forum* **777** 231–236
[39] Dutta R, Huizenga R, Gao H, Amirthalingam M, King A, Hermans M and Richardson I 2014 *Metallurgical and Materials Transactions A* **45** 5281–5285

[40] Ranjan R and Singh S B 2017 *Metallurgical & Materials Transactions A* **49** 88–93
[41] Xiong Z, Mitchell D R G, Saleh A A and Pereloma E V 2018 *Metallurgical & Materials Transactions A* **49** 5925–5929
[42] Rampelberg C, Allain S Y P, Geandier G, Teixeira J, Lebel F and Sourmail T 2021 *JOM* **73** 3183–3194
[43] Gaudez S, Teixeira J, Denis S, Geandier G and Allain S Y P 2022 *Materials Characterization* **185** 111740
[44] Forouzan F, Surki Aliabad R, Hedayati A, Hosseini N, Maawad E, Blasco N and Vuorinen E 2023 *Materials* **16** 1557
[45] Singh S B and Paliwal M 2025 *Journal of Materials Science* **60** 1726–1735
[46] Rementeria R, Dominguez-Reyes R, Capdevila C, Garcia-Mateo C and Caballero F G 2020 *Scientific Reports* **10** 1–6
[47] McLellan R B 1988 *Journal of Physics and Chemistry of Solids* **49** 1213–1217
[48] Bhadeshia H K D H 2021 *Theory of Transformations in Steels* (London, U.K.: CRC Press, Taylor and Francis Group)
[49] Bhadeshia H K D H and Edmonds D V 1980 *Acta Metallurgica* **28** 1265–1273
[50] Bhadeshia H K D H 2015 *Bainite in Steels: Theory and Practice* 3rd ed (Leeds, U.K.: Maney Publishing)
[51] Bhadeshia H K D H 1984 Solute-drag, kinetics and the mechanism of the bainite transformation *Phase Transformations in Ferrous Alloys* ed Marder A R and Goldstein J I (Ohio, USA: TMS-AIME) pp 335–340
[52] Wadley H N G and Mehrabian R 1984 *Materials Science & Engineering* **65** 245–263
[53] van Bohemen S M C, Hermans M J M, den Ouden G and Richardson I 2002 *Journal of Applied Physics D* **35** 1889–1894
[54] van Bohemen S M C, Hermans M J M, den Ouden G and Richardson I M 2003 *Journal de Physique IV* **112** 301–304
[55] van Bohemen S M C 2004 *An acoustic emission study of martensitic and bainitic transformations in carbon steel.* Ph.D. thesis Technical University of Delft The Netherlands
[56] van Bohemen S M C, Sietsma J, Hermans M J M and Richardson I M 2005 *Philosophical Magazine* **85** 1791–1804
[57] Wozniak T Z 2008 *Materials Characterization* **59** 708–716
[58] Wozniak T Z, Rozniatowski K and Ranachowski Z 2011 *Metals and Materials International* **17** 365–373
[59] Wozniak T Z, Jelenkowski J, Rozniatowski K and Ranachowski Z 2012 *Materials Science Forum* **726** 55–62
[60] Watson J D and McDougall P G 1973 *Acta Metallurgica* **21** 961–973
[61] Trafarski A, Łazarska M and Ranachowski Z 2021 *Bulletin of the Polish Academy of Sciences. Technical Sciences* **69** e139389
[62] Łazarska M, Piotrowska A, Paciorek-Sadowska J and Ranachowski Z 2024 *Polish Journal of Chemical Technology* **26** 34–38
[63] Kuba M M and van Aken D C 2013 *Metallurgical & Materials Transactions A* **44** 3444–3455
[64] Łazarska M, Ranachowski Z, Musiał J, Tański T and Jiang Q 2025 *Materials* **18** 2198
[65] van Bohemen S M C and Sietsma J 2014 *Materials Science and Technology* **30** 1024–1033
[66] Matsumura O, Sakuma Y and Takechi H 1987 *Transactions of the Iron and Steel Institute of Japan* **27** 570–579
[67] Matsumura O, Sakuma Y and Takechi H 1987 *Scripta Metallurgica* **27** 1301–1306
[68] Rundman K B and Klug R C 1982 *Transactions of the American Foundrymen Society* **90** 499–508
[69] Bhadeshia H K D H 2007 Steels for rails *Encyclopedia of Materials Science* (Pergamon Press, Oxford, Elsevier Science) pp 1–7

[70] Yates J K 1996 *Science in Parliament* **53** 2–3
[71] Bhadeshia H K D H 2005 *Materials Science and Technology* **21** 1293–1302
[72] Burian W, Marcisz J, Garbarz B and Starczewski L 2014 *Archives of Metallurgy and Materials* **59** 1211–1216
[73] Pramanick A K, Das H, Reddy G M, Ghosh M, Das G and Pal T K 2016 *Materials & Design* **103** 52–62
[74] Mishra B, Sukumar G, Senthil P, Reddy P, Singh B, Ramakrishna B, Kumar K S and Madhu V 2023 *Defence Science Journal* **73** 131–139
[75] Garbarz B, Marcisz J, Burian W, Kowalski A, Borowski J, Szkudelski S, Walicki M and Zajac K 2023 *Problems of Mechatronics. Armament, Aviation, Safety Engineering* **14** 23–60
[76] DeCooman B 2004 *Current Opinion in Solid State and Materials Science* **8** 285–303
[77] Jacques P J 2004 *Current Opinion in Solid State and Materials Science* **8** 259–265
[78] Bhadeshia H K D H 2002 *ISIJ International* **42** 1059–1060
[79] Bhadeshia H K D H and Edmonds D V 1983 *Metal Science* **17** 411–419
[80] Self P G, Bhadeshia H K D H and Stobbs W M 1981 *Ultramicroscopy* **6** 29–40
[81] Saha Podder A, Lonardelli I, Molinari A and Bhadeshia H K D H 2011 *Proceedings of the Royal Society A* **467** 3141–3156
[82] Garcia-Mateo C, Peet M, Caballero F G and Bhadeshia H K D H 2004 *Materials Science and Technology* **20** 814–818
[83] Fielding L C D, Jones N G, Walsh J, Boxel S V, Blackmur M S, Lee P D, Withers P J, Stone H J and Bhadeshia H 2016 *Acta Materialia* **105** 52–58